High-Affinity Inhibitors of Dihydrofolate Reductase: Antimicrobial and Anticancer Activities of 7,8-Dialkyl-1,3-diaminopyrrolo[3,2-*f*]quinazolines with Small Molecular Size

Lee F. Kuyper,*,† David P. Baccanari,† Michael L. Jones,† Robert N. Hunter,† Robert L. Tansik,† Suzanne S. Joyner,† Christine M. Boytos,† Sharon K. Rudolph,† Vince Knick,† H. Robert Wilson,† J. Marc Caddell,† Henry S. Friedman,‡ John C. W. Comley,§ and Jeremy N. Stables§

Wellcome Research Laboratories, Research Triangle Park, North Carolina 27709, Wellcome Research Laboratories, Beckenham, Kent BR3 3BS, U.K., and Duke University Medical Center, Durham, North Carolina 27710

Received July 13, 1995⊗

A series of 7,8-dialkylpyrrolo[3,2-*f*]quinazolines were prepared as inhibitors of dihydrofolate reductase (DHFR). On the basis of an apparent inverse relationship between compound size and antifungal activity, the compounds were designed to be relatively small and compact. Inhibitor design was aided by a GRID analysis of the three-dimensional structure of *Candida albicans* DHFR, which suggested that relatively small, branched alkyl groups at the 7- and 8-positions of the pyrroloquinazoline ring system would provide optimal interactions with a hydrophobic region of the protein. The compounds were potent inhibitors of fungal and human DHFR, with K_i values as low as 7.1 and 0.1 pM, respectively, and were highly active against *C. albicans* and an array of tumor cell lines. In contrast to known lipophilic inhibitors of DHFR such as trimetrexate and piritrexim, members of this series of pyrroloquinazolines were not susceptible to P-glycoprotein-mediated multidrug resistance and also showed significant distribution into lung and brain tissue. The compounds were active in lung and brain tumor models and displayed *in vivo* activity against *Pneumocystis carinii* and *C. albicans*.

Introduction

The enzyme dihydrofolate reductase (DHFR) is a known target for drug action.[1,2] Inhibitors of DHFR have proven useful in the treatment of cancer,[3−6] bacterial infections,[7] malaria,[8] and *Pneumocystis carinii* pneumonia (PCP).[9,10] Efforts to develop new therapies based on DHFR inhibition continue. One area of recent focus is the search for inhibitors of DHFR from various opportunistic organisms such as the protozoan parasite *Toxoplasma gondii* [11−13] and the fungus *Candida albicans*.[14] The importance of opportunistic diseases has risen considerably in recent years, owing to the large increase in the population of immunocompromised patients associated with the AIDS (acquired immune deficiency syndrome) epidemic, organ transplantation, and cancer chemotherapy.[15−17] Therapeutic intervention is limited by the dearth of safe and effective antiparasitic and antifungal agents.[17]

Another area of recent interest is the development of novel lipophilic DHFR inhibitors for neoplastic disease.[4] Although methotrexate (MTX, **1**) is effective against acute lymphocytic leukemia, non-Hodgkin's lymphoma, and osteosarcoma,[3,18] the hydrophilic nature of MTX restricts its distribution to various body tissues, such as lung and brain,[18] and prevents entry into cells by diffusion. Thus, the antitumor activity of MTX relies on the active transport of the drug into cancer cells,[19,20] and resistance to MTX can arise from impairment of this transport mechanism.[21]

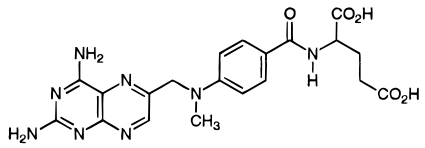

MTX, **1**

The lipophilic inhibitors metoprine (DDMP, **2**), piritrexim (PTX, **3**), and trimetrexate (TMX, **4**) were designed to avoid the limitations of MTX. DDMP, for example, concentrates in the brain relative to plasma and was evaluated as a potential treatment for brain tumors.[22] Both PTX and TMX are active against transport-impaired MTX-resistant cell lines and show tissue distribution profiles significantly different from that of MTX.[23,24] In addition, compounds PTX and TMX also exhibit clinical activity against *P. carinii*, an opportunistic fungal organism afflicting many AIDS patients.[25−28] As in many other fungal and bacterial species, folates are synthesized *de novo* by *P. carinii*, and the organism lacks the ability to take up folates from its environment. Thus, PTX and TMX can be given in combination with folinic acid (leucovorin), which is taken up only by the host cells and counteracts the antifolate toxicity of the drugs.[9,10]

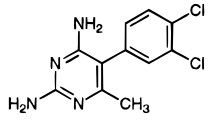

DDMP, **2**

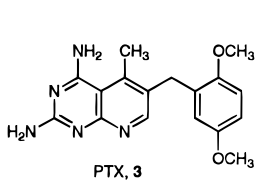

PTX, **3**

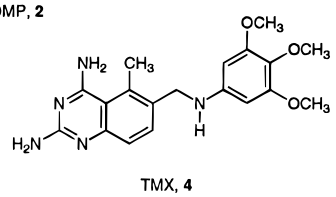

TMX, **4**

* To whom correspondence should be addressed. Current address: Glaxo Wellcome Inc., Five Moore Dr., Research Triangle Park, NC 27709.
† Wellcome Research Laboratories, NC.
‡ Duke University Medical Center.
§ Wellcome Research Laboratories, U.K.
⊗ Abstract published in *Advance ACS Abstracts,* January 15, 1996.

0022-2623/96/1839-0892$12.00/0

Scheme 1[a]

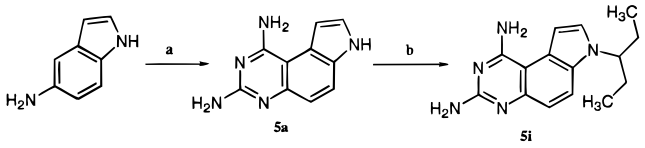

[a] Reagents and conditions: (a) $NaN(CN)_2$, 1-octanol, reflux, 13 h; (b) isopentyl tosylate, NaH, DMF.

This paper describes a series of lipophilic DHFR inhibitors that showed antimicrobial and anticancer activities and potentially advantageous tissue distribution properties. The compounds arose from an effort to identify DHFR inhibitors with useful activity against the fungus *C. albicans*. Initial attempts to identify lead compounds from our corporate collection of DHFR inhibitors were disappointing. Although a number of compounds showed significant inhibition of *C. albicans* DHFR (e.g., PTX and TMX), few displayed activity against *C. albicans in vitro*. Inconsistencies between the level of enzyme inhibition and antimicrobial activity were observed with other classes of inhibitors as well. As one working hypothesis, we speculated that antimicrobial activity might be inversely related to the molecular size of the inhibitor. That assumption led us to design a series of 7,8-dialkylpyrrolo[3,2-*f*]quinazolines **5** that were relatively small and compact but showed high affinity for DHFR. Inhibitor design was based on the three-dimensional structure of *C. albicans* DHFR and aided by the computer program GRID.[29] The resulting compounds were potent inhibitors of bacterial, fungal, protozoal, and human cells. Compared to PTX, TMX, and MTX, the new compounds displayed (1) substantially greater activity against human and fungal DHFR, (2) more effective growth inhibition of a number of tumor and fungal cell lines, (3) activity against cells with P-glycoprotein-mediated multidrug resistance, (4) superior tissue distribution properties for lung and brain tumor applications, (5) activity in murine models for brain and lung tumors, and (6) superior *in vivo* activity against *P. carinii* and *C. albicans*.

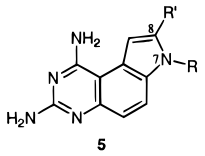

Chemistry

The preparation of 1,3-diamino-7*H*-pyrrolo[3,2-*f*]-quinazolines was originally reported by Ledig[30] and involved a thermally induced condensation of 5-aminoindole and dicyanamide. 7-Substituted analogues were prepared by alkylation of the parent pyrroloquinazoline or the intermediate indole. Our initial preparation of compound **5i**, for example, employed analogous procedures, alkylating with isopentyl tosylate as illustrated in Scheme 1. However, the low yields of the alkylation reactions and the need to explore a variety of 7,8-dialkylated analogues prompted us to develop alternative procedures. We also devised improved conditions for effecting the cyclization using boron trifluoride etherate.[31]

Scheme 2 outlines procedures employed in our improved synthesis of compounds **5**. The key 2,3-dialkyl-5-nitroindole intermediates **9** (Table 1) were obtained by one of two methods: (1) N-alkylation of 2-alkylindoles

Scheme 2[a]

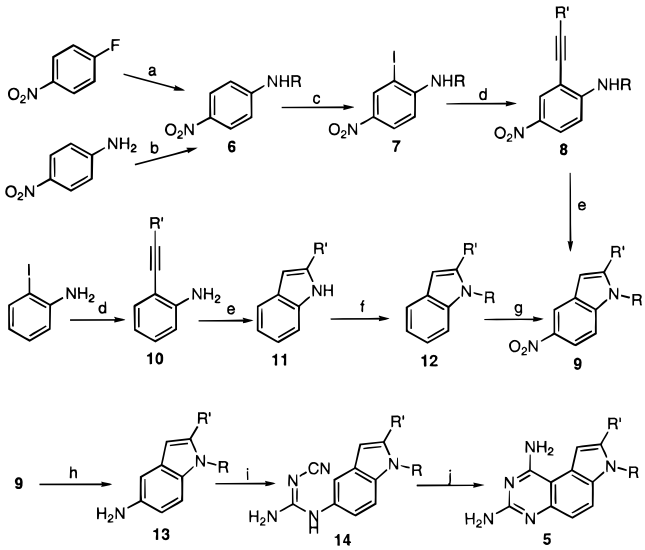

[a] Reagents and conditions: (a) H_2NR, DMSO, 50 °C; (b) ketone, $NaBH_3CN$, HCl, CH_3OH; (c) ICl; (d) alkyne, CuI, Et_3N, DMF, $Pd(PPh_3)_2Cl_2$; (e) CuI, DMF, reflux; (f) ROTs, NaH, DMF; (g) HNO_3, H_2SO_4; (h) H_2, Pd/C; (i) $NaN(CN)_2$, DMF; (j) refluxing diglyme or BF_3·etherate, DME.

11 using sodium hydride in DMF and the desired alkyl tosylate, followed by regioselective nitration, or (2) copper-catalyzed cyclization of 2-alkynyl-4-nitroanilines **8** (Table 2). The latter compounds were derived from the 4-nitro-*N*-alkylanilines **6** (Table 2), which were prepared from 4-nitroaniline via reductive alkylation[32,33] or from 4-fluoronitrobenzene by aromatic nucleophilic substitution with the appropriate alkylamine.[34,35] Iodination of the *N*-alkylanilines **6** was effected with ICl in methanol.[36,37] Introduction of the alkynyl moiety employed palladium catalysis,[38] and cyclization of the alkynylanilines **8** to the indoles **9** was performed with copper iodide.[39,40] Conversion of the nitroindoles **9** to the aminoindoles **13** was performed in high yield using catalytic hydrogenation.

Construction of the diaminopyrimidine ring followed our previously reported procedures for the preparation of the parent ring system.[31] The aminoindoles **13** were condensed with dicyanamide to give the cyanoguanidine derivatives **14** (Table 3), and ring closure to the target compounds **5** (Table 4) was carried out thermally or with boron trifluoride etherate. Synthesis of *tert*-butyl-substituted analogues **5f**,**l**,**p**,**r** was incompatible with the procedure employing BF_3·etherate but was effected successfully using thermal conditions.

Results and Discussion

Inhibitor Design. Hundreds of inhibitors of DHFR have been reported during the past several decades,[41] and most of the compounds that show high affinity for DHFR appear to make use of the large hydrophobic cleft observed in X-ray crystal structures of the enzyme from various species.[2,42−44] For example, PTX, a potential treatment for PCP,[10] binds to *P. carinii* DHFR with its dimethoxybenzyl group positioned within the large hydrophobic cavity of that enzyme.[45] As shown in Figure 1, the benzyl group of the inhibitor is surrounded by the side chains of Leu-25, Ile-33, Phe-36, Ile-65, Pro-66, Phe-69, and Leu-72.

Of particular pertinence to the work described here is a series of 7-substituted-pyrrolo[3,2-*f*]quinazolines

Table 1. Substituted Indoles[a]

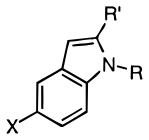

compd	X	R′	R	mp (°C)	yield[b] (%)	formula
9c	NO_2	Me	Me	128−129	79	$C_{10}H_{10}N_2O_2$
9d	NO_2	Et	Me	127−128	38	$C_{11}H_{12}N_2O_2$
9e	NO_2	*i*-Pr	H	151−152	73	$C_{11}H_{12}N_2O_2$
9f	NO_2	*t*-Bu	H	134−136	86	$C_{12}H_{14}N_2O_2$
9g	NO_2	Et	Et	84−85	42	$C_{12}H_{14}N_2O_2 \cdot 0.1H_2O$
9h	NO_2	Me	*i*-Pr	156−158	63	$C_{12}H_{14}N_2O_2$
9j	NO_2	*i*-Pr	Et	70−72	45	$C_{13}H_{16}N_2O_2$
9k	NO_2	*n*-Pr	Et	67−68	65	$C_{13}H_{16}N_2O_2$
9l	NO_2	Et	*t*-Bu	121−123	66	$C_{14}H_{18}N_2O_2$
9m	NO_2	Me	$C(Me)_2Et$	66−68	74	$C_{14}H_{18}N_2O_2$
9n	NO_2	Et	CH(Me)Et	63−64	81	$C_{14}H_{18}N_2O_2$
9o	NO_2	Me	$CHEt_2$	69−71	31	$C_{14}H_{18}N_2O_2$
9p	NO_2	*t*-Bu	*i*-Pr	125−126	95	$C_{15}H_{20}N_2O_2$
9q	NO_2	Et	$CHEt_2$	oil	92	$C_{15}H_{20}N_2O \cdot 0.1H_2O$
9r	NO_2	*n*-Bu	*t*-Bu	90−91	71	$C_{16}H_{22}N_2O_2$
9s	NO_2	*n*-Pr	$CHEt_2$	55−56	98	$C_{16}H_{22}N_2O_2$
9t	NO_2	*i*-Pr	$CHEt_2$	oil	92	$C_{16}H_{22}N_2O_2$
11e	H	*i*-Pr	H	72−73	69	$C_{11}H_{13}N$
11k	H	*n*-Pr	H	oil	81	$C_{11}H_{13}N$
12d	H	Et	Me	oil	60	$C_{11}H_{13}N$
12g	H	Et	Et	oil	46	$C_{12}H_{15}N \cdot 0.2$hexane
12h	H	Me	*i*-Pr	oil	26	$C_{12}H_{15}N$
12j	H	*i*-Pr	Et	oil	78	$C_{13}H_{17}N$
12k	H	*n*-Pr	Et	oil	90	$C_{13}H_{17}N$
12o	H	Me	$CHEt_2$	oil	50	$C_{14}H_{19}N$
13c	NH_2	Me	Me	>250	92	$C_{10}H_{12}N_2 \cdot HCl$
13d	NH_2	Et	Me	220−221	100	$C_{11}H_{14}N_2 \cdot HCl$
13f	NH_2	*t*-Bu	H	>250	100	$C_{12}H_{16}N_2 \cdot HCl$
13g	NH_2	Et	Et	175−176	93	$C_{12}H_{16}N_2 \cdot HCl$
13h	NH_2	Me	*i*-Pr	230−231	100	$C_{12}H_{16}N_2 \cdot 0.25EtOH \cdot 0.2HCl$
13j	NH_2	*i*-Pr	Et	230−231	96	$C_{13}H_{18}N_2 \cdot HCl$
13k	NH_2	*n*-Pr	Et	185−186	98	$C_{13}H_{18}N_2 \cdot HCl$
13o	NH_2	Me	$CHEt_2$	175−176	96	$C_{14}H_{20}N_2 \cdot HCl$

[a] All compounds were characterized by ^1H NMR, mass spectra, and elemental analyses. Other compounds in these series were not purified for analytical purposes and were characterized only by ^1H NMR spectra. [b] Yields were not optimized.

first reported by Ledig.[30] Those compounds are inhibitors of mammalian and bacterial DHFR[46] and show *in vitro* activity against the *C. albicans* organism.[47] Molecular modeling suggested that this class of inhibitor binds to DHFR with the 7-substituent occupying the large hydrophobic cleft in a manner similar to the dimethoxybenzyl group of PTX; those compounds with larger 7-substituents generally displayed higher affinity for *C. albicans* DHFR. For example, compound **5u** was comparable to PTX and TMX in its inhibition of the fungal enzyme (see Table 5). However, the inhibitors with the larger substituents were relatively ineffective inhibitors of *C. albicans* growth. Thus the challenge was to reduce inhibitor size and yet retain tight enzyme binding, and the design problem was to identify small substituents for the pyrroloquinazoline heterocycle that would impart high affinity for DHFR. The relatively potent activity reported for 7-(cyclopropylmethyl)-2,4-diaminopyrrolo[3,2-*f*]quinazoline suggested that small alkyl substituents can impart high affinity for DHFR[46] and effective inhibition of *C. albicans* cell growth.[47] Further exploration of such small alkyl substituents was aided by the use of GRID, a computer program that evaluates the interaction between a protein active site and a variety of probe functions.[29] A crystal structure of the *C. albicans* holoenzyme was furnished by Whitlow and co-workers,[48] and a methyl group probe was used in GRID to analyze the binding site. As illustrated in Figure 2, regions of favorable interaction energy for a methyl group, formed by Met-25, Ile-33, Phe-36, Met-54, Ile-62, and Leu-69, were adjacent to the 7- and 8-positions of enzyme-bound pyrroloquinazoline. The area next to the 8-position was relatively small and centered in the plane of the inhibitor's ring system. Small, branched alkyl groups at the 8-position appeared to take good advantage of that site. On the other hand, the 7-position of the pyrroloquinazoline was positioned at the edge of the large hydrophobic cavity of the protein, and favorable binding locations for the methyl probe were found close to the parent inhibitor but above and below the plane of the pyrroloquinazoline ring system. Substituents such as the 3-pentyl group that would adopt conformations that are perpendicular to the pyrroloquinazoline ring system, as shown in Figure 2, were required to position methyl groups into regions

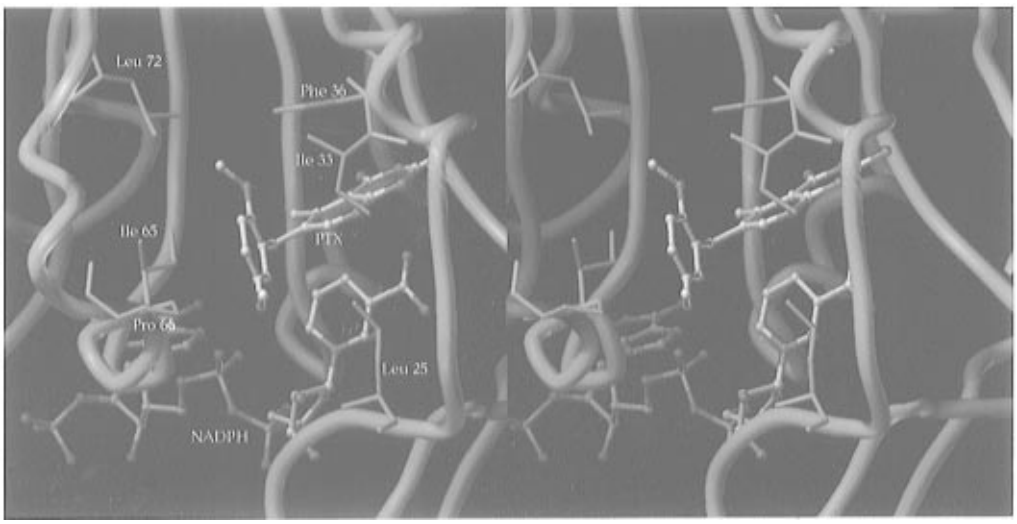

Figure 1. Stereoview of the active site region of the X-ray crystal structure of the *P. carinii* DHFR−NADPH−piritrexim complex. The protein backbone is represented as a dark pink tube, and and atoms of selected residues are shown. Atoms of piritrexim and NADPH are colored by atom type: carbon, white; nitrogen, cyan; oxygen, red; and phosphorus, orange.

Table 2. Substituted Anilines[a]

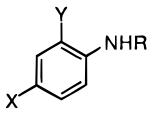

compd	X	Y	R	mp (°C)	yield[b] (%)	formula
6h	NO_2	H	*i*-Pr	82−84	92	$C_9H_{12}N_2O_2$
6l	NO_2	H	*t*-Bu	68−69	84	$C_{10}H_{14}N_2O_2$
6m	NO_2	H	$C(Me)_2Et$	oil	67	$C_{11}H_{16}N_2O_2$
6n	NO_2	H	CH(Me)Et	oil	89	$C_{10}H_{14}N_2O_2$
6o	NO_2	H	$CHEt_2$	oil	83	$C_{11}H_{16}N_2O_2$
7h	NO_2	I	*i*-Pr	52−53	67	$C_9H_{11}N_2O_2I$
7l	NO_2	I	*t*-Bu	115−116	71	$C_{10}H_{13}N_2O_2I$
7m	NO_2	I	$C(Me)_2Et$	oil	81	$C_{11}H_{15}N_2O_2I$
7n	NO_2	I	CH(Me)Et	oil	76	$C_{10}H_{13}N_2O_2I$
7o	NO_2	I	$CHEt_2$	oil	71	$C_{11}H_{15}N_2O_2I$
8l	NO_2	−C≡C−Et	*t*-Bu	131−132	89	$C_{14}H_{18}N_2O_2$
8m	NO_2	−C≡C−Me	$C(Me)_2Et$	oil	95	$C_{14}H_{18}N_2O_2$
8n	NO_2	−C≡C−Et	CH(Me)Et	oil	98	$C_{14}H_{18}N_2O_2$
8o	NO_2	−C≡C−Me	$CHEt_2$	oil	85	$C_{14}H_{18}N_2O_2 \cdot 0.2H_2O$
8q	NO_2	−C≡C−Et	$CHEt_2$	oil	99	$C_{15}H_{20}N_2O_2$
8r	NO_2	−C≡C−Bu	*t*-Bu	oil	90	$C_{16}H_{22}N_2O_2$
10e	H	−C≡C−*i*-Pr	H	oil	94	$C_{11}H_{13}N$
10k	H	−C≡C−*n*-Pr	H	oil	91	$C_{11}H_{13}N$

[a] All compounds were characterized by ^{1}H NMR, mass spectra, and elemental analyses. Other compounds in these series were not purified for analytical purposes and were characterized only by ^{1}H NMR spectra. [b] Yields were not optimized.

Table 3. *N*-Cyano-*N′*-(1,2-dialkylindol-5-yl)guanidines[a]

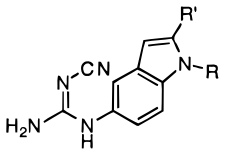

compd	R′	R	mp (°C)	yield (%)[b]	formula
14c	Me	Me	215−216	89	$C_{12}H_{13}N_5$
14i	H	$CHEt_2$	68−69	47	$C_{15}H_{19}N_5$
14k	*n*-Pr	Et	195−196	86	$C_{15}H_{19}N_5$
14n	Et	CH(Me)Et	135−137	57	$C_{16}H_{21}N_5$
14o	Me	$CHEt_2$	151−152	97	$C_{16}H_{21}N_5$
14q	Et	$CHEt_2$	145−147	37	$C_{17}H_{23}N_5$
14r	*n*-Bu	*t*-Bu	127−128	67	$C_{18}H_{25}N_5$

[a] All compounds were characterized by elemental analyses, ^{1}H NMR, and mass spectra. Other compounds in this series were not purified for analytical purposes and were characterized only by ^{1}H NMR spectra. [b] Yield was not optimized.

indicated by the GRID analysis. On the basis of this simple analysis, the series of 7,8-dialkylpyrrolo[3,2-*f*]-quinazolines listed in Table 4 were prepared.

***In Vitro* Biological Activities.** The series of 7,8-dialkylpyrrolo[3,2-*f*]quinazolines **5a**−**u** were evaluated as inhibitors of *C. albicans* and human DHFR and for growth inhibition of fungal and human cells. As shown in Table 5, several members of the series displayed exceptional affinity for DHFR and potent inhibition of cell growth. DHFR K_i values were as low as 7.1 pM against *C. albicans* DHFR and 0.1 pM for the human enzyme. Compound concentrations effective against whole cells ranged as low as 1 ng/mL for *C. albicans* and 0.57 nM for the human colon tumor cell line HCT-8. Potent activity was also observed against bacteria. For example, compound **5o** inhibited *Escherichia coli* with a minimum inhibitory concentration (MIC) of 0.1 ng/mL.

In this series of pyrroloquinazolines, only the parent compound **5a** and its 7-methyl derivative **5b** were less active than PTX and TMX as inhibitors of *C. albicans* DHFR. Activity against the fungal enzyme increased substantially with additional alkyl substitution at either the 7- or 8-position. The compound with the lowest measured K_i value (**5m**, K_i 7.1 pM) was 3200-fold more active than its parent compound **5a** and more than 260-fold more active than PTX and TMX. Alkyl substitution at the 8-position of the pyrroloquinazoline ring system enhanced activity significantly. An 8-methyl group provided a 12-fold increase in affinity for the fungal enzyme (**5c** versus **5b**), and isopropyl substitution increased activity more than 140-fold (**5e** versus **5a**). Tertiary butyl and *n*-propyl groups also fit into the fungal enzyme binding pocket (compounds **5f**,**k**,**p**,**s**), but, as suggested by the molecular modeling experiments, the binding pocket imposed a substituent size limit at the 8-position. The *n*-butyl group appeared to encounter those limits; compound **5r** was significantly less active than the corresponding ethyl-substituted analogue **5l**. The enzyme active site imposed fewer restrictions on size for substituents at the 7-position of the pyrroloquinazoline ring system, as exemplified by the trimethoxybenzyl group of compound **5u** (and also the large substituents of PTX and TMX). However, the GRID analysis suggested that smaller 7-substituents with appropriate shape could contribute significantly to binding. This was verified by compound **5i**; its 3-pentyl group provided a contribution to enzyme affinity (K_i 0.22 nM) equivalent to that of the much larger trimethoxybenzyl group of compound **5u** (K_i 0.23 nM). A combination of small, compact alkyl substituents at the 7- and 8-positions provided inhibitors with exceptional affinity for the fungal enzyme (compounds **5l**−**q**,**s**,**t**).

The effects of 7- and 8-alkyl substituents on affinity for human DHFR were similar to those observed for the fungal enzyme. The most active pyrroloquinazoline inhibitors, compounds **5l**−**q**,**s**,**t**, displayed K_i values in the sub-picomolar range and were significantly more active than PTX and TMX. For reference purposes, the most potent pyrroloquinazolines were also 1 order of magnitude more active than MTX (K_i 1.3 pM), the bench-mark hydrophilic anticancer agent.[3] No evidence for substitution patterns that might selectively favor

Table 4. 7,8-Disubstituted-1,3-diaminopyrrolo[3,2-*f*]quinazolines[a]

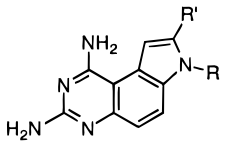

compd	R′	R	mp (°C)	yield (%)[b]	formula
5a[c]	H	H	264−266	64	$C_{10}H_9N_5$
5b[c]	H	Me	248−250	18	$C_{11}H_{11}N_5 \cdot 0.6H_2O$
5c	Me	Me	303−305	38	$C_{12}H_{13}N_5 \cdot 0.5H_2O$
5d	Et	Me	>250	57	$C_{13}H_{15}N_5$
5e	*i*-Pr	H	>250	20	$C_{13}H_{15}N_5 \cdot 0.2EtOAc \cdot 0.3H_2O$
5f	*t*-Bu	H	>250	21	$C_{14}H_{17}N_5 \cdot 0.5H_2O$
5g	Et	Et	227−229	36	$C_{14}H_{17}N_5 \cdot 0.95H_2O$
5h	Me	*i*-Pr	150−160	42	$C_{14}H_{17}N_5 \cdot 0.7H_2O$
5i	H	$CHEt_2$	197−198	47	$C_{15}H_{19}N_5 \cdot 0.9H_2O$
5j	*i*-Pr	Et	217−219	20	$C_{15}H_{19}N_5$
5k	*n*-Pr	Et	239−241	41	$C_{15}H_{19}N_5 \cdot 0.1H_2O$
5l	Et	*t*-Bu	200−202	65	$C_{16}H_{21}N_5$
5m	Me	$C(Me)_2Et$	254−256	28	$C_{16}H_{21}N_5$
5n	Et	CH(Me)Et	199−200	37	$C_{16}H_{21}N_5 \cdot 0.7H_2O$
5o	Me	$CHEt_2$	200−201	33	$C_{16}H_{21}H_5 \cdot 0.25H_2O$
5p	*t*-Bu	*i*-Pr	286−287	65	$C_{17}H_{23}N_5 \cdot 0.2H_2O$
5q	Et	$CHEt_2$	155−157	60	$C_{17}H_{23}N_5 \cdot H_2O$
5r	*n*-Bu	*t*-Bu	233−234	23	$C_{18}H_{25}N_5 \cdot$TFA
5s	*n*-Pr	$CHEt_2$	121−122	64	$C_{18}H_{25}N_5$
5t	*i*-Pr	$CHEt_2$	243−244	30	$C_{18}H_{25}N_5 \cdot 0.5H_2O$
5u[c]	H	3,4,5-trimethoxybenzyl	242−243	46	$C_{20}H_{21}N_5O_3 \cdot 0.5H_2O$

[a] All compounds were characterized by ^{1}H NMR, mass spectra, and elemental analyses. [b] Yield was not optimized. [c] Originally reported in ref 30.

Table 5. Biological Data for 7,8-Disubstituted-1,3-diaminopyrrolo[3,2-*f*]quinazolines

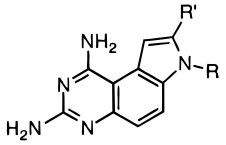

compd	R′	R	MW	*C. albicans* DHFR K_i (nM)[a]	human DHFR K_i (pM)[a]	*C. albicans* MIC (μg/mL)	HCT-8 IC_{50} (nM)
PTX			325	1.9	25*	>10	68
TMX			369	1.9	1.4*	>50	1.8
5a	H	H	199	23	1000	0.8	1450
5b	H	Me	213	25	230	1.6	580
5c	Me	Me	227	2.0	87	0.1	85
5d	Et	Me	241	1.3	29	0.1	8.0
5e	*i*-Pr	H	241	0.16	10	0.05	
5f	*t*-Bu	H	255	0.12*	<2.0	0.05	3.3
5g	Et	Et	255	0.33	10	0.2	0.59
5h	Me	*i*-Pr	255	0.22	6.4	0.025	7.4
5i	H	$CHEt_2$	269	0.22	4.5	0.001	6.0
5j	*i*-Pr	Et	269	0.33	<2.0	0.1	1.4
5k	*n*-Pr	Et	269	0.65	24	0.1	3.1
5l	Et	*t*-Bu	283	<0.05	0.1*	>0.1	1.3
5m	Me	$C(Me)_2Et$	283	0.0071*	0.4*	0.025	2.1
5n	Et	CH(Me)Et	283	<0.05	0.1*	0.1	0.82
5o	Me	$CHEt_2$	283	0.030*	0.3*	0.025	0.74
5p	*t*-Bu	*i*-Pr	297	<0.06	0.2*	0.05	1.3
5q	Et	$CHEt_2$	297	<0.06	0.2*	0.1	0.57
5r	*n*-Bu	*t*-Bu	311	0.38	30	>0.1	52
5s	*n*-Pr	$CHEt_2$	311	<0.11	0.4*	>0.1	4.4
5t	*i*-Pr	$CHEt_2$	311	<0.05	0.1*	>0.1	0.75
5u	H	3,4,5-trimethoxybenzyl	379	0.23	6.0*	5.0	

[a] Values marked with an asterisk were measured directly. Otherwise, values were calculated from the IC_{50} value.

inhibition of the fungal enzyme versus human DHFR emerged from this series of pyrroloquinazolines.

A number of the alkyl-substituted pyrroloquinazolines were potent inhibitors of *C. albicans* growth. However, the level of growth inhibition did not correlate with DHFR K_i. For example, the trimethoxybenzyl-substituted pyrroloquinazoline **5u** weakly inhibited *C. albicans* growth (MIC 5 μg/mL). In contrast, compound **5i**, which exhibited a fungal enzyme K_i essentially identical with that of analogue **5u**, was 5000-fold more active than **5u** against the organism *in vitro*. The majority of pyrroloquinazolines showed *C. albicans* MICs within a narrow range (0.025−0.1 μg/mL), but those compounds had fungal DHFR K_i values that differed up to 280-fold. The working hypothesis that antifungal activity might be related to the molecular size of the inhibitor was not

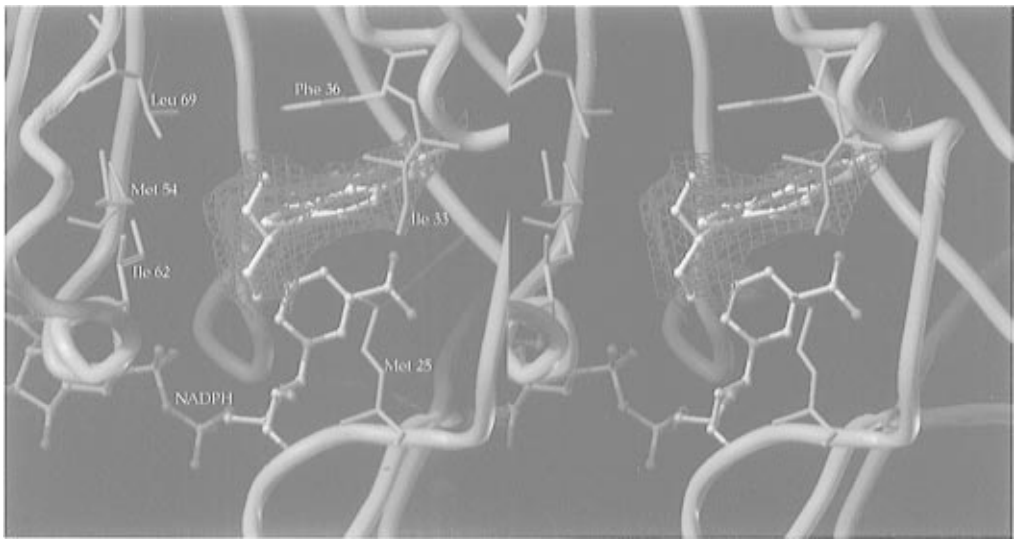

Figure 2. Stereoview of the active site region of the X-ray crystal structure of the *C. albicans* DHFR−NADPH−compound **5i** complex. The green mesh represents the −1.5 kcal/mol isoenergy contour surface from GRID. The surface was calculated using coordinates of the holoenzyme and a methyl group probe. Molecule representation is as described in Figure 1.

Table 6. Cytotoxicities of Compounds **5i**,**o** Compared to MTX, PTX, and TMX (IC_{50}, nM)

cell line	**5i**	**5o**	MTX	PTX	TMX
P388D1	4.5	0.12	4.8	21	2.7
L cells	2.2	0.6	8.3	76	4.7
D54		4.6	16	230	60
143B(TK$^-$)		0.8	8.8		
U87MG	8	2.1	22	48	11
A549	10	0.4	31	24	5.3
H460		0.5	9.5	260	
Daoy	80	2.3	9.0	70	12
U373MG		2.3	12	55	9.6
Vero		1.0	9.2	30	16

Table 7. Comparative IC_{50} Values against Normal and Multidrug-Resistant Cell Lines

	relative IC_{50} for compound[a]					
cell line	VBL	ADR	PTX	TMX	**5i**	**5o**
KB3-1	1	1	1	1	1	1
KBV-1	2000	61	16	20	1.1	1
KBV-1 + reserpine	1.3	1.6	1.5	1.5	1.1	0.8
MCF7	1	1	1	1	1	1
MCF7/ADR	17500	200	6.8	8.6	0.9	0.9
MCF7/ADR + reserpine	0.5	1.5	0.8	1.2	0.7	0.6
P388D1	1	1	1	1		1
P388/ADR	19	28	3.7	8.9		0.8
P388/ADR + reserpine	0.2	3.7	0.3	0.3		0.9

[a] The IC_{50} values were normalized to that observed for the parent sensitive cell line for each compound.

supported by our observations; analysis of data from almost 100 pyrroloquinazolines did not reveal any distinct relationships between activity and inhibitor size and/or lipophilicity.

Unlike the poor correlation between *C. albicans* DHFR K_i and *C. albicans* MIC, the activities of the compounds in Table 5 against HCT-8 tumor cells were highly correlated with human DHFR K_i values (r^2 = 0.97). The most potent pyrroloquinazoline inhibitor of HCT-8 cells, compound **5q**, was 3-fold more active than TMX.

Compounds **5i**,**o** were subjected to further *in vitro* and *in vivo* studies. In comparison to PTX, TMX, and MTX, compound **5o** showed superior activity against an array of human and murine cell lines, as shown in Table 6. The average cytotoxicity of compound **5o** was approximately 10-fold greater than that of MTX and TMX and 50-fold greater than that of PTX.

Susceptibility to Multiple Drug Resistance. Cell lines KBV-1, MCF7/ADR, and P388/ADR, which express the multiple drug resistance phenotype (MDR), are resistant to adriamycin (ADR), vinblastine (VBL), and a number of structurally unrelated antitumor agents. The resistance stems from the action of a membrane-bound glycoprotein (P-glycoprotein) that actively effluxes cytotoxic agents by an energy-dependent mechanism.[49,50] Reserpine is a reversing agent that blocks the efflux activity of P-glycoprotein and restores sensitivity of MDR cells to ADR and VBL.[51] The lipophilic DHFR inhibitors PTX and TMX also are susceptible to the MDR phenotype,[52] whereas the hydrophilic DHFR inhibitor MTX is not.[53] In contrast to PTX and TMX, compounds **5i**,**o** were equally effective against both the parent and MDR cell lines, and their cytotoxicity was not affected by reserpine (Table 7). Since acquired MDR and normal expression of P-glycoprotein in tumors derived from tissues such as colon, small intestine, kidney, and liver are important problems in cancer therapy, a compound such as **5o** could have broad therapeutic applications.

The small molecular size of **5i**,**o** may play a role in their lack of susceptibility to P-glycoprotein-mediated MDR. The degree of susceptibility to MDR was quantitatively related to molecular weight for a series of unrelated anticancer agents by Selassie et al.[54] Moreover, the high activity of compounds **5o**,**i** against *C. albicans* may be linked to their poor activity as substrates for the mammalian P-glycoprotein efflux pump. A relative of *C. albicans*, *Saccharomyces cerevisiae*, expresses a protein with high homology to human P-glycoprotein[55] that mediates the transmembrane transport of an endogenous peptide.[56] The presence of a P-glycoprotein in a fungal organism suggests the possibility that fungi might also use such proteins for protection against cytotoxic agents. The MDR susceptibilities and activities against *C. albicans* of PTX, TMX, and compounds **5i**,**o** were consistent with this idea.

Another possible benefit for compounds not affected by MDR involves tissue distribution. P-Glycoprotein is found in normal tissues such as liver, kidney, and colon and also is expressed in endothelial cells at the blood−

Table 8. Tissue Distribution of Compounds **5i**,**o** Compared to MTX, DDMP, PTX, and TMX

	relative level compared to plasma	
compd	brain	lung
5i[a]	10	57
5o[a]	10	50
MTX[b]	0.006	0.05
PTX[a]	0.65	5.5
TMX[a]	0.1	
DDMP[c]	6.5	31

[a] Studies were performed in mice. At time of tissue collection, plasma drug concentration of **5i** was 0.4 μg/mL, compound **5o** was 0.4 μg/mL, PTX was 3.5 μg/mL, and TMX was 9.4 μg/mL. [b] Rabbits received high-dose MTX (70 mg/kg) by infusion; steady-state plasma MTX concentration was 160 μg/mL.[79] [c] Rats received 1 mg/kg DDMP po; tissues were collected 5 h postdose; plasma DDMP concentration was 0.6 μg/mL.[22]

brain barrier.[57] Lack of drug distribution into these tissues, especially the brain, is a common limitation for treatment of tumors and fungal infections, and drug distribution properties may, in part, be related to susceptibility to the P-glycoprotein efflux pump. PTX amd TMX do not distribute significantly into the brain.[58] However, smaller DHFR inhibitors with similar lipophilicity, such as pyrimethamine and metoprine, do achieve substantial concentrations in brain tissue and are not substrates for P-glycoprotein.[58] Tissue distribution properties of compounds **5i**,**o** are described below.

Tissue Distribution Studies. Therapy with MTX, PTX, and TMX is limited by the tissue distribution properties of these compounds. They do not readily cross the blood−brain barrier and do not attain high lung concentrations relative to plasma (Table 8). Compounds **5i**,**o** exhibited greatly improved brain/plasma and lung/plasma concentration ratios and, thus, may be useful against lung and brain tumors. DDMP also concentrated in the brain and lung. However, clinical trials with DDMP revealed central nervous system (CNS), cutaneous, and gut toxicities[59] that may be related to inhibition of histamine metabolism.[60] A therapeutic dose of compound **5o** (10 mg/kg, sc) did not elevate brain histamine above control levels (20 ng/mL) in mice, whereas DDMP (10 mg/kg, ip) elevated brain histamine to 100 ng/mL for 15 h postdose.

***In Vivo* Antitumor Studies.** The high brain/plasma and lung/plasma concentration ratios of compounds **5i**,**o** and their *in vitro* activity against MDR-expressing cell lines suggested the compounds may be active against brain, lung, and MDR tumors *in vivo*.

Several therapy experiments were performed with P388 leukemia cells in mice. MTX, PTX, ADR, and compounds **5i**,**o** produced significant increases in life span in mice with ip implants of P388 cells (Table 9). Compound **5o**, when administered ip, showed antitumor activity in mice with intraperitoneal implants of MDR cell line P388/ADR comparable to that in mice with implants of the parent P388 tumor line. The sensitivity of the p388/ADR implants to compound **5o** was reduced in a second experiment in which the compound was given sc.

Compounds **5i**,**o** were more active than MTX or PTX against intracranially (ic) implanted P388. However, compound **5o** was inactive when tested against ic implants of other tumor lines, including D54 glioma, U87MG glioma, and 143B(TK$^-$) osteosarcoma cells. Since these tumor cell lines were sensitive to inhibition by compound **5o** in *in vitro* cytotoxicity assays (Table 6), the reason for inactivity in these brain tumor models is not known.

In vivo studies with compound **5o** were extended to lung tumor models. Therapy with compound **5o** (10 mg/kg, sc) reduced the number of lung tumor nodules by 68% with no significant toxicity in mice with intrathoracic (it) implants of human A549 non-small-cell lung carcinoma (NSCLC). The activity of compound **5o** approached that of mitomycin C (4 mg/kg, nodule reduction 92%), whereas MTX (2 mg/kg) was inactive in this model. However, compound **5o** did not increase the life span of mice with it implants of A549 cells or another NSCLC line (NCI H460).

Antifungal and Antiprotozoal Studies. Compound **5o** was a potent, though nonselective, inhibitor of DHFR from *T. gondii* and *P. carinii*. The inhibitory potency of compound **5o** against *T. gondii* DHFR (K_i 0.9 nM) was 300-fold greater than that of pyrimethamine (K_i 300 nM). Pyrimethamine, in combination with sulfonamides, is clinically effective in the treatment of toxoplasmosis.[61,62] In an *in vitro T. gondii* plaque reduction assay, compound **5o** (MIC 0.00025 μg/mL) was 2000-fold more potent than pyrimethamine (MIC 0.5 μg/mL) (R. Berens, University of Colorado Health Sciences Center). In comparison, the MIC value of TMX was 0.01 μg/mL. Leucovorin (25 μM) did not reverse the *in vitro* activity of compound **5o** against *T. gondii*.

Compound **5o** was a potent inhibitor of *P. carinii* DHFR (IC_{50} 14 nM), comparable to PTX (IC_{50} 32 nM) and TMX (IC_{50} 66 nM) and considerably more active than trimethoprim (IC_{50} 24 μM),[63] three agents that are clinically active against PCP.[9,10,64,65] PTX and TMX, like compound **5o**, are not selective for *P. carinii* DHFR, and leucovorin must be coadministered to prevent antifolate-related toxicity in patients. We compared the activity of compound **5o**/leucovorin to that of PTX/leucovorin and trimethoprim/sulfamethoxazole (TMP/SMX) against PCP in *SCID* mice (Table 10). PTX/leucovorin had no effect on the extent of the infection, whereas significant reductions in the intensity of the infection were seen with both TMP/SMX and compound **5o**/leucovorin. The superior activity of compound **5o** compared to PTX may reflect the enhanced distribution of compound **5o** to lungs.

Compounds **5i**,**o** were potent nonselective inhibitors of *C. albicans* DHFR and the *C. albicans* organism *in vitro*, with MICs of 0.001 and 0.025 μg/mL, respectively (Table 5). These compounds were evaluated in murine models of *Candida* nephritis with concomitant meningitis. The infection level in the brain 48 h after inoculation with *C. albicans* was ca. 10^5 colony forming units (cfu)/g of tissue in vehicle- or SMX-treated control mice (Table 11). Treatment with compound **5o** reduced brain infection levels 10-fold, consistent with the observation that **5o** distributed to brain. Compound **5o** also was efficacious against candidal nephritis. In vehicle- or SMX-treated mice, greater than 10^7 cfu/g were recovered from kidney tissue. Treatment with compound **5o** alone led to a 7200-fold reduction of fungi in the kidney, and in mice treated with the combination of compound **5o** and SMX, infection levels were 44 000-fold lower than those of control mice. Compound **5i** also was active in this model but to a lesser degree.

In conclusion, the relatively small, lipophilic DHFR inhibitors described here showed a variety of interesting properties in comparison to known inhibitors. In con-

Table 9. Effect of Compounds **5i**,**o** and MTX, PTX, and ADR on Life Span of Mice with Intraperitoneally and Intracranially Implanted P388 Leukemic Cells

	increase in life span (%)		
compd	P388 (ip[a])	P388/ADR (ip[a])	P388 (ic[a])
5i (40 mg/kg, sc)	80 ($n = 8$)		40−55[b] ($n = 22$)
5o (10 mg/kg, sc)	80 ($n = 8$)	20 ($n = 8$)	27−50[c] ($n = 32$)
5o (12.5 mg/kg, sc)	90 ($n = 8$)	30 ($n = 8$)	60 ($n = 8$)
5o (10 mg/kg, ip)	38 ($n = 5$)	50 ($n = 5$)	
ADR	69−130[d] ($n = 13$)	8−30[c] ($n = 13$)	
PTX	40 ($n = 8$)	−5 ($n = 8$)	0 ($n = 10$)
MTX	115 ($n = 8$)	130 ($n = 8$)	0−15[d] ($n = 14$)

[a] Implant site: ip, intraperitoneal; ic, intracranial. [b] Results from three separate experiments. [c] Results from four separate experiments. [d] Results from two separate experiments.

Table 10. Comparison of Compound **5o**, PTX, and Trimethoprin against *P. carinii* Pneumonia in *SCID* Mice

	infection score[a]		no. of mice	statistical
treatment	mean	SEM[b]	infected/total[c]	significance[d]
D_5W ip and sc (control)	3.0	0.13	11/11	
leucovorin	3.0	0.26	11/11	
5o + leucovorin	0.18	0.11	2/11	B, C
PTX + leucovorin	3.27	0.13	11/11	A
TMP + SMX	0.9	0.17	8/10	B

[a] Infection scores: 0 = no infection evident; 1 = very weak infection; 2 = mild infection; 3 = moderate infection; 4 = heavy infection. [b] Standard error of mean. [c] Total number of mice at end of experiment. [d] A, not significantly different ($P < 0.05$) from results for the controls and leucovorin alone; B, significantly different ($P < 0.05$) from results for the controls; C, significantly different ($P < 0.05$) from results for TMP + SMX.

Table 11. Effect of Compounds **5i**,**o** on *C. albicans* Nephritis and Meningitis in Immunosuppressed Mice

	log cfu/g of tissue[a]	
compd	brain	kidney
vehicle control	5.1 ± 0.2	7.1 ± 0.1
5i	nd	6.0
5o	3.6 ± 0.3	3.4
SMX	4.7	7.3 ± 0.1
5i + SMX	nd	4.6
5o + SMX	3.4	2.5 ± 0.1

[a] Values are averages of duplicate experiments, with the range indicated. Those values without a range are from single experiments.

trast to PTX and TMX, the new compounds were potent inhibitors of *C. albicans* cell growth, were not susceptible to P-glycoprotein-mediated MDR, distributed significantly into lung and brain tissue, were active in murine models for lung and brain tumors, and showed superior *in vivo* activity against *P. carinii* and *C. albicans*.

Experimental Section

Chemistry. ^{1}H NMR spectra were recorded on Varian XL-200 and XL-300 spectrometers. Chemical shifts are in parts per million (δ), relative to the observed solvent resonance (DMSO, 2.50). Mass spectra were determined by Oneida Research Services (Whitesboro, NY) on a Finnegan 4500 instrument. Analytical samples of intermediates moved as single spots on TLC (Whatman MK6F silica gel plates). Column chromatography was carried out on silica gel 60 (E. Merck, Darmstadt, Germany). Melting points were determined with a Thomas-Hoover melting point apparatus and are uncorrected. Analyses were performed by Atlantic Microlab, Inc., Atlanta, GA, and all values are within 0.4% of theory. Octanol/water partition coefficients were measured by Midwestern Research Institute. The pK_a of compound **5o** was determined using ultraviolet methods as described for related compounds.[66] A sample of TMX was generously provided by the National Cancer Institute.

2-(1-Pentynyl)aniline (10k). To a mixture of 8.8 g (40 mmol) of 2-iodoaniline (Aldrich), 150 mg (0.21 mmol) of bis-(triphenylphosphine)palladium(II) chloride, and 35 mg (0.18 mmol) of CuI in 250 mL of triethylamine was added 7.0 mL (70 mmol) of 1-pentyne. The mixture was stirred under nitrogen at room temperature for 48 h. Solvent was removed *in vacuo*, and the residue was taken up in 400 mL of diethyl ether. The mixture was filtered through Celite, and the filtrate was dried over $MgSO_4$. Removal of solvent on a rotary evaporator left a dark residue, which was subjected to flash chromatography (silica gel, 95:5 hexanes:ethyl acetate) to give 5.8 g (91%) of compound **10k** as an oil: ^{1}H NMR ($CDCl_3$) 7.25 (m, 1H), 7.10 (m, 1H), 6.65 (m, 2H), 3.90 (br s, 2H), 2.45 (t, 2H, $J = 7$ Hz), 1.65 (dt, 2H, $J = 7$ Hz), 1.05 (t, 3H, $J = 7$ Hz); MS (CI) M + 1, 160 (100). Anal. ($C_{11}H_{13}N$) C, H, N.

2-Propylindole (11k). A mixture of 3.8 g (24 mmol) of compound **10k**, 15 mg (7.9 mmol) of CuI, and 100 mL of DMF was kept at reflux under nitrogen for 4 h. The mixture was stirred at room temperature for 16 h and concentrated to dryness. The residue was taken up in diethyl ether and filtered through Celite. The filtrate was subjected to flash chromatography (silica gel, 49:1 hexanes:ethyl acetate) to furnish 3.0 g (81%) of **11k** as an amber oil: ^{1}H NMR ($CDCl_3$) 7.80 (br s, 1H), 7.55 (m, 1H), 7.30 (m, 1H), 7.3 (m, 1H), 7.2−7.0 (m, 2H), 6.25 (br s, 1H), 2.7 (t, $J = 7$ Hz, 2H), 1.75 (dt, $J = 7$, 7 Hz, 2H), 1.05 (t, $J = 7$ Hz, 3H); MS (CI) M + 1, 160 (100). Anal. ($C_{11}H_{13}N$) C, H, N.

***N*-Ethyl-2-propylindole (12k).** To a mixture of 2.4 g (0.1 mol) of NaH (97%) in 100 mL of DMF was added 8.0 g (0.050 mmol) of compound **11k**. The mixture was stirred at room temperature for 0.5 h, and 8.0 mL (0.11 mol) of bromoethane was added dropwise. The mixture was stirred for 1 h and concentrated on a rotary evaporator. Methanol was added cautiously to the residue, and the mixture was concentrated to dryness. The residue was partitioned between diethyl ether and water. The ether layer was washed with water and dried over $MgSO_4$. Removal of solvent on a rotary evaporator left 8.49 g (90%) of **12k** as an amber oil: ^{1}H NMR ($CDCl_3$) 7.60 (d, $J = 7$ Hz, 1H), 7.35 (d, $J = 7$ Hz, 1H), 7.25−7.10 (m, 2H), 6.30 (s, 1H), 4.20 (q, $J = 6$ Hz, 2H), 2.75 (t, $J = 6$ Hz, 2H), 1.85 (m, 2H), 1.40 (t, $J = 6$ Hz, 3H), 1.1 (t, $J = 6$ Hz, 3H); MS (CI) M + 1, 188 (100). Anal. ($C_{13}H_{17}N$) C, H, N.

***N*-Ethyl-2-propyl-5-nitroindole (9k).** To an ice bath-cooled solution of 8.0 g (43 mmol) of **12k** in 450 mL of H_2SO_4 was added dropwise a solution of 4.0 g (47 mmol) of $NaNO_2$ in 50 mL of H_2SO_4. The solution was stirred at 0 °C for 5 h and at room temperature for 12 h. The mixture was poured onto ice and stirred for 0.75 h. The resulting precipitate was collected by filtration and dissolved in ethyl acetate. The organic solution was washed with saturated $NaHCO_3$ and water and dried over $MgSO_4$. Solvent was removed *in vacuo*, and the residue was subjected to flash chromatography (silica gel, 9:1 hexanes:ethyl acetate) to provide 6.40 g (65%) of **9k** as a white solid: mp 67−68 °C; ^{1}H NMR (DMSO-d_6) 8.4 (s, 1H), 7.95 (dd, $J = 8$, 3 Hz, 1H), 7.6 (d, $J = 8$ Hz, 1H), 6.5 (s, 1H), 4.2 (q, $J = 7$ Hz, 2H), 2.7 (t, $J = 7$ Hz, 2H), 1.7 (dt, $J = 7$, 7 Hz, 2H), 1.25 (t, $J = 7$ Hz, 3H), 1.0 (t, $J = 7$ Hz, 3H); MS M + 1, 233 (100). Anal. ($C_{13}H_{16}N_2O_3$). C, H, N.

1,3-Diamino-7-(1-ethylpropyl)-7*H*-pyrrolo[3,2-*f*]quinazoline (5i). A suspension of 180 g (2.04 mol) of 3-pentyl alcohol, 1 L of methylene chloride, 600 mL of pyridine, and 307 g (1.62 mol) of *p*-toluenesulfonyl chloride was stirred for 24 h. A solution of 300 mL of concentrated hydrochloric acid in 1 L of water was cautiously added to the reaction mixture. The

mixture was stirred for 2 h, and the methylene chloride layer was separated. The water layer was extracted with diethyl ether, and the extractions were combined with the methylene chloride layer. The volume of the organic solution was reduced to 500 mL on a rotary evaporator and washed with 0.1 N hydrochloric acid until the aqueous layer remained acidic. The organic layer was then washed thoroughly with water, dried ($MgSO_4$), and filtered, and the solvent was removed *in vacuo* to give 230 g (60%) of 1-ethylpropyl 4-toluenesulfonate as a white solid: mp 44−45 °C; HPLC (Nova Pak C18, 70% MeOH/H_2O/0.1% Et_3N/0.1% TFA) K' 2.67; ^1H NMR ($CDCl_3$) 7.8 (d, J = 7 Hz, 2H), 7.3 (d, J = 7 Hz, 2H), 4.45 (p, J = 5 Hz, 1H), 2.4 (s, 3H), 1.6 (m, 4H), 0.8 (t, J = 7 Hz, 6H). Anal. ($C_{12}H_{18}O_3S$) C, H.

A suspension of 18.0 g (89.8 mmol) of compound **5a**[31] in 800 mL of dry DMF was stirred under nitrogen while 4.0 g (170 mmol) of ca. 97% sodium hydride was added. The mixture was stirred for 1 h, and a solution of 24 g (99 mmol) of 1-ethylpropyl 4-toluenesulfonate in 80 mL of dry DMF was added dropwise over a period of 30 min. Stirring was continued for 8 h, and solvent was removed *in vacuo*. The dark residue was dissolved in 300 mL boiling methanol. The solution was treated with charcoal and filtered through Celite. The resulting dark solution was boiled down to 200 mL and allowed to cool. The resulting crystalline solid was isolated by filtration and washed with two 50-mL portions of cold methanol, sonicated with 200 mL of 0.1 N sodium hydroxide, and filtered. The solid was then washed with two 50-mL portions of water and dried *in vacuo* to afford 12.5 g (52%) of compound **5i** as an off-white solid: mp 197−198 °C; ^1H NMR (DMSO-d_6) 7.80 (d, J = 9 Hz, 1H), 7.51 (d, J = 3 Hz, 1H), 7.07 (d, J = 3 Hz, 1H), 7.02 (d, J = 9 Hz, 1H), 6.62 (br s, 2H), 5.62 (s, 2H), 4.32 (m, 1H), 1.85 (m, 4H), 0.64 (t, J = 7 Hz, 6H); λ_{max} (0.1 N HCl) 342 (ϵ 11 208), 230 (ϵ 26 874), 257 sh (ϵ 18 339) nm; λ_{min} 284 (ϵ 846), 219 (ϵ 22 396) nm; HPLC (Nova Pak C18, 30% MeOH/H_2O with 0.1% TEA, 0.1% TFA) t_R 5.38 min. Anal. ($C_{15}H_{19}N_5 \cdot H_2O$) C, H, N.

***N*-(1-Ethylpropyl)-4-nitroaniline (6o).** A solution of 4-nitroaniline (13.8 g, 0.099 mol) and 12 N HCl (10 mL) in 200 mL of methanol was treated with a solution of 3-pentanone (14.5 mL, 0.144 mol) in methanol (15 mL) and stirred for 1 h at room temperature. The reaction mixture was then cooled in an ice bath, and a solution of sodium cyanoborohydride (8.7 g, 0.138 mol) in methanol (35 mL) was added at such a rate that the reaction temperature remained below 20 °C. The reaction mixture was stirred at room temperature for 2 h and basified with 10% NaOH (70 mL). The mixture was partially concentrated *in vacuo* to remove most of the methanol and diluted to 350 mL total volume with water. The aqueous solution was extracted with two 250-mL portions of ether, and the combined extracts were dried ($MgSO_4$) and concentrated to give an oil. Chromatography on silica gel (40% hexane/CH_2Cl_2) provided 17.3 g (84%) of compound **6o** as an orange oil: ^1H NMR ($CDCl_3$) 8.06 (d, J = 9 Hz, 2H), 6.50 (d, J = 9 Hz, 2H), 4.20−4.30 (br s, 1H), 3.30−3.40 (m, 1H), 1.40−1.70 (m, 4H), 0.94 (t, J = 7 Hz, 6H). Anal. ($C_{11}H_{16}N_2O_2$) C, H, N.

***N*-(1-Ethylpropyl)-2-iodo-4-nitroaniline (7o).** A mixture of compound **6o** (10.4 g, 0.0499 mol) and 20 mL of concentrated HCl in 150 mL of H_2O was heated to 50 °C and treated dropwise over 1 h with a solution of ICl (17 g, 0.1047 mol) in concentrated HCl (30 mL). The mixture was stirred at 50 °C for 2.5 h, cooled in an ice bath, and treated with Na_2SO_4 (10 g). The solution was stirred for 10 min at room temperature, diluted with 125 mL of diethyl ether, and stirred an additional 20 min. The aqueous layer was extracted with ether (100 mL), and the combined organic extracts were washed with saturated $NaHCO_3$ solution (100 mL), dried ($MgSO_4$), and concentrated *in vacuo* to leave an oil. The oil was subjected to flash chromatography on silica gel (33% hexane/CH_2Cl_2) to give 15.59 g of an orange oil. Distillation ($bp_{0.25}$ = 170−172 °C) provided 11.86 g (71%) of compound **7o** as a yellow oil: ^1H HMR ($CDCl_3$) 8.57 (d, J = 3 Hz, 1H), 8.10 (dd, J = 3, 9 Hz, 1H), 6.47 (d, J = 9 Hz, 1H), 4.80 (br d, 1H), 3.40 (m, 1H), 1.50−1.75 (m, 4H), 0.96 (t, J = 7 Hz, 6H). Anal. ($C_{11}H_{15}N_2O_2I$) C, H, N.

***N*-(1-Ethylpropyl)-2-propynyl-4-nitroaniline (8o).** 1-Propyne (2.7 mL, 48 mmol) was condensed and added to a cold solution of 4.0 g (12 mmol) of compound **7o** in 150 mL of triethylamine in a Parr pressure reaction vessel. To this solution was added 0.030 g (0.16 mmol) of CuI and 0.10 g (0.14 mmol) of bis(triphenylphosphine)palladium(II) chloride, and the pressure vessel was then sealed. The mixture was stirred at room temperature for 20 h. The solvent was removed *in vacuo*, and the residue was suspended on silica gel. The silica gel suspension of the residue was placed on a silica gel column and eluted with 10% ethyl acetate in hexanes to provide 2.5 g (85%) of compound **8o** as a yellow oil: ^1H NMR (DMSO-d_6) 7.98 (s, 1H), 7.90 (s, 1H), 6.75 (d, J = 9 Hz, 1H), 5.8 (d, J = 9 Hz, 1H), 3.5 (m, 1H), 2.1 (s, 3H), 1.5 (m, 4H), 0.8 (t, J = 7 Hz, 6H). Anal. ($C_{14}H_{18}N_2O_2 \cdot 0.2H_2O$) C, H, N.

5-Nitro-2-methyl-1-(1-ethylpropyl)indole (9o). A suspension of 2.5 g (10 mmol) of compound **8o** and 0.20 g (0.11 mmol) of copper iodide in 200 mL of DMF was refluxed for 5 h. Solvent was removed *in vacuo* to leave a dark residue, which was taken up in methanol. Silica gel was added, and solvent was removed *in vacuo*. The silica gel suspension of the residue was placed on a silica gel column and eluted with 5% ethyl acetate in hexane to furnish 2.25 g (90%) of compound **9o** as an oil: ^1H NMR (DMSO-d_6) 8.4 (m, 1H), 7.9 (br d, 1H), 7.7 (d, 1H), 6.5 (br s, 1H), 4.2 (m, 1H), 1.8−2.2 (m, 4H), 0.6 (t, 6H). Anal. ($C_{14}H_{18}N_2O_2$) C, H, N.

5-Amino-2-methyl-1-(1-ethylpropyl)indole Hydrochloride (13o). A mixture of compound **9o** (2.5 g, 10 mmol) in 100 mL of methanol and 10% palladium on carbon (0.3 g) was subjected to hydrogenation on a Parr apparatus (40 psi). When uptake of hydrogen ceased (ca. 2 h), the reaction mixture was filtered through Celite and 12 N HCl (3 mL) was added to the filtrate. The filtrate was concentrated to dryness. The residue was taken up in ethanol, and the solution was again concentrated to dryness. This sequence was repeated several times to remove excess HCl and left 2.5 g (97%) of compound **13o** as a white solid: mp 175 °C dec; HPLC (Nova Pak C18, 60% MeOH/H_2O, 0.1% Et_3N/0.1% TFA) K' 2.50; ^1H NMR (DMSO-d_6) 10.1 (s, 3H), 7.6 (d, J = 9 Hz, 1H), 7.4 (d, J = 2 Hz, 1H), 6.9 (dd, J = 2, 9 Hz, 1H), 6.3 (s, 1H), 4.1 (br s, 1H), 2.4 (s, 3H), 1.8−2.2 (m, 4H), 0.62 (t, J = 7 Hz, 6H). Anal. ($C_{14}H_{20}N_2 \cdot HCl$) C, H, N, Cl.

***N*-Cyano-*N'*-(2-methyl-1-(1-ethylpropyl)indol-5-yl)guanidine (14o).** A suspension of compound **13o** (2.4 g, 9.5 mmol) and sodium dicyanamide (2.5 g, 28 mmol) in 125 mL of DMF was heated to 50 °C for 4 h. Solvent was removed *in vacuo*, water (ca. 250 mL) was added, and the mixture was stirred for 1 h. Filtration furnished 2.7 g (100%) of compound **14o** as a tan solid: mp 151−152 °C; ^1H NMR (DMSO-d_6) 8.85 (s, 1H), 7.44 (d, J = 9 Hz, 1H), 7.34 (s, 1H), 6.84 (d, J = 9 Hz, 1H), 6.80 (s, 2H), 6.17 (s, 1H), 4.05 (m, 1H), 2.38 (s, 3H), 1.79−2.19 (m, 4H), 0.64 (t, 6H). Anal. ($C_{16}H_{21}N_5$) C, H, N.

1,3-Diamino-7-(1-ethylpropyl)-8-methyl-7*H*-pyrrolo-[3,2-*f*]quinazoline (5o). Method A. A mixture of 278 g (0.98 mol) of compound **14o** and 3.5 L of diglyme was kept at reflux for 20.5 h. The mixture was cooled slowly to 30 °C and filtered. The filter cake was washed with warm diglyme, and the combined filtrates were subjected to flash chromatography on silica gel, eluting with ethyl acetate:ethanol, 9:1. Fractions containing product were combined and concentrated to a thick slurry which was stirred with cooling (ice/water bath) for 1 h. The slurry was filtered, and the off-white filter cake was washed with cold ethanol and dried *in vacuo* at 45 °C overnight. A slurry of the solid in 1.2 L of 1 N NaOH was stirred overnight, and the solid was isolated by filtration. Recrystallization from DMSO, followed by a thorough water wash, provided 46.2 g (17%) of compound **5o** as a white solid: mp 198−199 °C; ^1H NMR (DMSO-d_6) 7.76 (d, J = 9.2 Hz, 1H), 6.90 (d, J = 9.2 Hz, 1H), 6.78 (s, 1H), 6.58 (s, 2H), 5.64 (s, 2H), 4.10 (m, 1H), 2.42 (s, 3H), 2.10 (m, 2H), 1.88 (m, 2H), 0.62 (t, J = 7.2 Hz, 6H); MS (CI) M + 1 (100). Anal ($C_{16}H_{21}N_5 \cdot 0.7H_2O$) C, H, N.

Method B. A suspension of compound **14o** (2.6 g, 9.2 mmol) in 300 mL of methanol was placed in a Parr pressure reactor and heated to 150 °C for 35 h. The reaction mixture was cooled, and solvent was removed *in vacuo*. The residue was subjected to chromatography on silica gel, eluting with 10% EtOH in CH_2Cl_2. The resulting solid was sonicated with 200 mL of 0.1 N NaOH for 1 h. The mixture was filtered, and the

solid was dried *in vacuo* to yield 0.87 g (33%) of compound **5o** as an off-white solid: mp 200−201 °C. Anal. ($C_{16}H_{21}N_5$·0.25 H_2O) C, H, N.

Method C. To a mixture of 510 g (1.80 mol) of compound **14o** and 2.5 L of 1,2-dimethoxyethane under nitrogen was added 664 mL (766 g, 5.4 mol) of BF_3·Et_2O while the temperature was maintained at ≤45 °C (ice/water bath). The mixture was stirred overnight at room temperature and then concentrated on a rotary evaporator. The residual dark oil was dissolved in a minimum amount of methanol and added to 5 L of NH_4OH. The resulting slurry was stirred vigorously overnight. The solid was isolated by filtration, washed with water, and dried *in vacuo* at 40 °C overnight. This crude material was subjected to flash chromatography on silica gel, eluting with 9:1 ethyl acetate:ethanol containing 1% NH_4OH. The purified material was slurried overnight in 1 N NaOH (1.5 L) and filtered. The filter cake was washed with water and dried *in vacuo* at 50 °C. Recrystallization from DMSO, followed by extensive washing with water, provided 184 g (36%) of compound **5o** as an off-white solid: mp 188−189 °C. Anal. ($C_{16}H_{21}N_5$·0.3H_2O·0.1DMSO) C, H, N, S. The measured log *P* (octanol/water) of compound **5o** was 3.0. The pK_a of compound **5o** was 8.1, and its log *D* measured at pH 7.4 was 2.4.

The methanesulfonate salt of compound **5o**, which had significantly greater water solubility than the free base, was prepared as follows. A solution of 3.0 g (10 mmol) of compound **5o** in 100 mL of methanol was added dropwise to a solution of 0.74 mL (1.1 g, 11 mmol) of methanesulfonic acid in 100 mL of methanol. The solution was stirred at room temperature for 1 h, and solvent was removed *in vacuo*. The light brown residue was triturated with diethyl ether and recrystallized twice from 5:1 diethyl ether:methanol to furnish 2.85 g (73%) of the methanesulfonate salt of compound **5o** as a tan solid: mp 157−158 °C; ^{1}H NMR (DMSO-d_6) 12.2 (s, 1H), 8.8 (s, 1H), 8.1 (d, J = 8.8 Hz, 1H), 7.6 (br s, 1H), 7.5 (br s, 2H), 7.1 (m, 2H), 4.2 (m, 1H), 2.4 (s, 3H), 1.8−2.2 (m, 4H), 0.6 (t, J = 7.5 Hz, 6H). Anal. ($C_{17}H_{25}N_5SO_3$) C, H, N, S.

Biology. Dihydrofolate reductase from *C. albicans* was prepared as previously described[14] and assayed in 0.1 M imidazole chloride buffer (pH 6.4), with 70 μM NADPH and 45 μM dihydrofolate in a final volume of 1 mL at 30 °C. Recombinant human DHFR (from Anatrace, Maumee, OH) was assayed in 50 mM sodium phosphate, pH 7.0. For determinations of IC_{50} values (the concentration of inhibitor necessary to inhibit enzymatic activity by 50%), the enzyme, NADPH, and varying concentrations of inhibitor were preincubated for 2 min, and the reaction was initiated by dihydrofolate. Steady-state velocities were measured, and plots of logarithm of inhibitor concentration versus percent inhibition were used to estimate IC_{50} values; coefficients of variation for IC_{50} values were <10%. For weak-binding compounds, K_i values were calculated from IC_{50} using Cha's equation for competitive inhibitors.[67] The Henderson method[68] as described by Baccanari and Joyner[69] was used for determining K_i values for tight-binding inhibitors; coefficients of variation between replicate assays were <20%. Dihydrofolate K_m values for *C. albicans* and human DHFR are 2.7 and 0.036 μM, respectively.[14,70] Compounds were tested as inhibitors of dihydrofolate reductase from *P. carinii* as previously described.[63] *T. gondii* DHFR inhibition was measured under the conditions used for *P. carinii* DHFR, except that substrate concentrations were 52 μM dihydrofolate and 73 μM NADPH.

T. gondii cell-free extracts were prepared from frozen *T. gondii* tachyzoites (stripped of human fibroblasts) supplied by Dr. R. Berens of the University of Colorado.[71] Briefly, 2.1 × 10^9 organisms were suspended in 1.5 mL of 50 mM PIPES (pH 6.8) and 0.1 M KCl at 4 °C and lysed with six 10-s bursts from a Vibracell sonifier (Sonics & Materials, Inc.). After centrifugation for 60 min at 39000*g* at 4 °C, the supernatant was collected and loaded onto a Sephadex G-25 column (1 × 8 cm). Fractions containing DHFR activity (eluting near the void volume of the column) were pooled and stored at −70 °C.

For growth inhibition assays, mammalian cells were adapted to and maintained in folic acid-free RPMI-1640 (GIBCO BRL) containing 10 nM (6*R*,*S*)-5-formyltetrahydrofolic acid and 10% fetal bovine serum (HyClone) that had been charcoal-dialyzed. In experiments measuring reversal of multiple drug resistance, 5 mM reserpine was used as a reversing agent. Cytotoxicity measurements were carried out in 96-well microtiter plates using the 3-(4,5-dimethylthiazol-2-yl)-2,5-diphenyltetrazolium bromide (MTT) dye reduction assay[72] for suspension cultures or the sulforhodamine B assay[73] for monolayer cultures. Cell lines A549 (human non-small-cell lung carcinoma), Daoy (human medulloblastoma), U87MG and U373MG (human glioblastomas), HCT-8 (human ileocecal adenocarcinoma), 143B(TK^-) (thymidine kinase-deficient human osteosarcoma), Vero (African green monkey kidney), and P388D1 (mouse lymphoid neoplasm) and mouse L cells were obtained from ATCC. Human large cell lung carcinoma NCI H460 was from the Southern Research Institute. P388/ADR was obtained from D. W. Fry at Parke-Davis Warner-Lambert. The vinblastine-resistant KBV-1 and its parent line KB3-1 (human epidermoid carcinoma) were obtained from the laboratory of M. Gottesman, National Institute of Health (via A. C. King, Wellcome Research Laboratories). The adriamycin-resistant MCF7/ADR10 was from the laboratory of R. Fine (Veterans Administration Medical Center, Durham, NC); the sensitive MCF7 cell line, conditioned to folate-free media, was from D. Duch (Wellcome Research Laboratories).

The *in vitro T. gondii* plaque reduction assay was performed as described by Ou-Yang et al.[74]

Intrathoracic tumor cell implants were performed in nude mice (NCr-nu/nu or Swiss) essentially as described by McLemore and co-workers.[75] Approximately 1 × 10^6 cells/mouse were implanted in anesthetized mice on day 0. Mice (10/group) were treated with compound **5o** (10 mg/kg) dissolved in 5% dextrose/water and administered sc daily on days 1−10, the maximum tolerated dose of MTX (2 mg/kg) dissolved in 2% $NaHCO_3$ and administered ip daily on days 1−9, or mitomycin C (4 mg/kg) dissolved in saline and administered ip on days 1, 5, and 9. In experiments with A549 NSCLC, mice were sacrificed on day 40, and antitumor activity was assessed by comparing the number of tumor foci on the lungs and thoracic cavity of control mice (36 and 48 foci/mouse in two separate experiments) to those of treated mice. In experiments with intrathoracic implants of other tumor cell lines, the median survival of drug-treated animals was compared to that of saline-treated controls.

For the D54 glioma, U87MG glioma, and 143B(TK^-) osteosarcoma brain tumor models, 1−2 × 10^6 cells (5−10 μL) were implanted intracranially essentially as described by Wang et al.[76] Mice were treated intraperitoneally with 5% dextrose in distilled water (D_5W) or compound **5o** (10−15 mg/kg) in D_5W qd × 10. Efficacy was measured by increase in life span, compared to controls.

The ic and ip studies with P388 utilized viral antibody-free CDF-1 female mice (18−20 g, 5 or 8/group) from Charles River (Portage, MI). P388, a murine leukemia cell line, was maintained *in vivo* by limited serial passage. Tumor cells were implanted intraperitoneally (1 × 10^6 cells) or intracranially (1 × 10^5 cells), and treatment was begun 24 h later. Compounds **5i** (40 mg/kg) and **5o** (12.5 mg/kg) were suspended in 0.5% carboxymethyl cellulose plus 1% Tween 80 and administered sc or ip qd × 10. MTX (4 mg/kg) was given ip qd × 9, PTX (40 mg/kg) ip q7h × 2 on days 1−5; and ADR (5 mg/kg) ip on days 1, 5, and 9.

Full details of the PCP model in *SCID* mice were recently reported.[77,78] Briefly, each drug or control group consisted of 10−11 mice. Drugs were evaluated for prophylaxis by administration once a day from day 1 postinfection for a total of 42 doses. Compound **5o** (20 mg/kg) and PTX (12 mg/kg, the estimated maximum tolerated dose) were dissolved in D_5W and administered ip followed 30 min later by leucovorin (in D_5W) dosed sc 12 mg/kg. Controls received D_5W ip and sc. Trimethoprim (50 mg/kg) and sulfamethoxazole (250 mg/kg) suspension was given orally. Mice received 0.1 mL of drug suspension/20 g of body weight. Twenty-four hours after the last drug dose, the presence of *P. carinii* in lung impression smears was rapidly and unambiguously identified by immunofluorescence. The intensity of the PCP was graded by scanning the impression smears and assigning, on a semilogarithmic basis, an infection score described in a footnote to Table 10. Results are presented as the calculated mean infection scores (±stan-

dard error of mean, SEM) and the ratio of the number of mice infected with *P. carinii* over the total number of mice remaining in each group at the end of the experiment. Since the data did not follow a pattern of normal distribution, a nonparametric test (Mann−Whitney *U* test) was used to compare the infection score between selected individual groups in the same drug study.

In vivo antifungal activity was assayed in a model of *Candida* nephritis. Nephritis was established in immunosuppressed CD-1 female mice (10/group) by inoculation of 5×10^4 cfu/mouse into the lateral tail vein. Immunosuppression was maintained by ip injection of 160 and 40 mg/kg cyclophosphamide on days −4 and −1, prior to inoculation, respectively. Treatment with compounds **5i**,**o** was by subcutaneous injection of 20 or 50 mg/kg, respectively, in 0.1 mL of sesame oil at 3, 7, 24, and 30 h, postinoculation. When used, sulfamethoxazole (200 mg/kg, ip, in D_5W) was administered 1 h prior to each compound dose. Efficacy was measured by culture of the kidneys and brain at 48 h postinoculation. After the tissues were ground, diluted in saline, plated, and incubated for 48 h, colonies were counted and the cfu/g of tissue was determined.

Tissue distribution of DHFR inhibitors was determined in male CD-1 mice (5/group). Compounds **5i**,**o** (60 mg/kg) were administered sc, and tissues were harvested at 3 and 1 h postdose, respectively. PTX (200 mg/kg) and TMX (100 mg/kg) were administered ip, and tissues were harvested 40 min postdose. At time of sacrifice, blood was drawn, the plasma was separated and frozen, and brains and lungs were removed and stored at −20 °C. Tissues were homogenized in 0.1 N HCl (in methanol) and centrifuged at 12000*g* for 30 min at 4 °C. The supernatants and plasma samples were prepared for analysis by solid phase extraction on C2 BondElut columns (Analytichem International). Drug concentrations were determined by HPLC on a Waters C18 μBondaPak column in 0.1 M ammonium acetate buffer at pH 4.0 with a 0−60% acetonitrile gradient. Brain histamine levels were measured with a histamine radioimmunoassay kit from Immunotech International.

Acknowledgment. We thank J. Champness for crystal structure coordinates of the *P. carinii* DHFR−NADPH−piritrexim complex. Determinations of pK_a were performed by D. Minick. We thank G. Martin, L. Taylor, and their respective staffs for NMR and mass spectrometric measurements and L. Elwell for the determination of antibacterial activities.

References

(1) Schweitzer, B. I.; Dicker, A. P.; Bertino, J. R. Dihydrofolate reductase as a therapeutic target. *FASEB J.* **1990**, *4*, 2441−2452.
(2) Kuyper, L. F. Inhibitors of dihydrofolate reductase. In *Computer-Aided Drug Design*; Perun, T. J., Propst, C. L., Eds.; Marcel Dekker Inc.: New York, 1989; pp 327−369.
(3) Bertino, J. R. Karnofsky Memorial Lecture: Ode to methotrexate. *J. Clin. Oncol.* **1993**, *11*, 5−14.
(4) Fleming, G. F.; Schilsky, R. L. Antifolates: The next generation. *Semin. Oncol.* **1992**, *19*, 707−719.
(5) Sirotnak, F. M., Burchall, J. J., Ensminger, W. B., Montgomery, J. A., Eds. *Folate Antagonists as Therapeutic Agents*; Academic Press: New York, 1984.
(6) Roth, B.; Cheng, C. C. Recent progress in the medicinal chemistry of 2,4-diaminopyrimidines. In *Progress in Medicinal Chemistry*; Ellis, G. P., West, G. B., Eds.; Elsevier Biomedical Press: Amsterdam, 1982; Vol. 19, pp 269−331.
(7) Salter, A. J. Trimethoprim-sulfamethoxazole: An assessment of more than 12 years of use. *Rev. Infect. Dis.* **1982**, *4*, 196−236.
(8) Hitchings, G. H. The metabolism of plasmodia and the chemotherapy of malarial infections. In *Tropical Medicine from Romance to Reality*; Wood, C., Ed.; Academic Press: London, 1978; pp 79−98.
(9) Allegra, C. J.; Chabner, B. A.; Tuazon, C. U.; Ogata-Arakaki, D.; Baird, B.; Drake, J. C.; Simmons, J. T.; Lack, E. E.; Shelhamer, J. H.; Balis, F.; Walker, R.; Kovacs, J. A.; Lane, H. C.; Masur, H. Trimetrexate for the treatment of *Pneumocystis carinii* pneumonia in patients with the acquired immunodeficiency syndrome. *N. Engl. J. Med.* **1987**, *317*, 978−985.
(10) Falloon, J.; Allegra, C.; Kovacs, J.; O'Neill, D.; Ogata-Arakaki, D.; Feuerstein, I.; Polis, M.; Davey, R.; Lane, H. C.; LaFon, S.; Rogers, M.; Zunich, K.; Zurlo, J.; Tuazon, C.; Parenti, D.; Simon, G.; Masur, H. Piritrexim with leucovorin for the treatment of pneumocystis pneumonia (PCP) in AIDS patients. *Clin. Res.* **1990**, *38*, 361A.
(11) Rosowsky, A.; Hynes, J. B.; Queener, S. F. Structure-activity and structure-selectivity studies on diaminoquinazolines and other inhibitors of *Pneumocystis carinii* and *Toxoplasma gondii* dihydrofolate reductase. *Antimicrob. Agents Chemother.* **1995**, *39*, 79−86.
(12) Kovacs, J. A.; Allegra, C. J.; Masur, H. Characterization of dihydrofolate reductase of *Pneumocystis carinii* and *Toxoplasma gondii*. *Exp. Parasitol.* **1990**, *71*, 60−68.
(13) Derouin, F.; Chastang, C. In vitro effects of folate inhibitors on *Toxoplasma gondii*. *Antimicrob. Agents Chemother.* **1989**, *33*, 1753−1759.
(14) Baccanari, D. P.; Tansik, R. L.; Joyner, S. S.; Fling, M. E.; Smith, P. L.; Freishheim, J. H. Characterization of *Candida albicans* dihydrofolate reductase. *J. Biol. Chem.* **1989**, *264*, 1100−1107.
(15) Edwards, J. E. Invasive Candida infections. Evolution of a fungal pathogen. *N. Engl. J. Med.* **1991**, *324*, 1060−1062.
(16) Leoung, G., Mills, J., Eds. *Opportunistic Infections in Patients with the Acquired Immunodeficiency Syndrome*; Marcel Dekker: New York, 1989.
(17) Sternberg, S. The emerging fungal threat. *Science* **1994**, *266*, 1632−1634.
(18) Jolivet, J.; Cowan, K. H.; Curt, G. A.; Clendeninn, N. J.; Chabner, B. A. The pharmacology and clinical use of methotrexate. *N. Engl. J. Med.* **1983**, *309*, 1094−1104.
(19) Dembo, M.; Sirotnak, F. M. Membrane transport of folate compounds in mammalian cells. In *Folate Antagonists as Therapeutic Agents*; Sirotnak, J. M., Burchall, J. J., Ensminger, W. B., Montgomery, J. A., Eds.; Academic Press: New York, 1984; Vol. 1, pp 173−217.
(20) Henderson, G. B. Transport of folate compounds into cells. In *Nutritional, Pharmacologic and Physiologic Aspects of Folates and Pterins*; Blakeley, R. I., Whitehead, M. V., Eds.; Wiley: New York, 1986; pp 207−250.
(21) Sirotnak, F. M. Determinants of resistance to antifolates: Biochemical phenotypes, their frequency of occurence and circumvention. *Natl. Cancer Inst. Monogr.* **1987**, *5*, 27−35.
(22) Cavallito, J. C.; Nichol, C. A.; Brenckman, W. D., Jr.; Deangelis, R. L.; Stickney, D. R.; Simmons, W. S.; Sigel, C. W. Lipid-soluble inhibitors of dihydrofolate reductase I. Kinetics, tissue distribution, and extent of metabolism of pyrimethamine, metoprine, and etoprine in the rat, dog, and man. *Drug Metab. Dispos.* **1978**, *6*, 329−337.
(23) Sigel, C. W.; Macklin, A. W.; Woolley, J. L., Jr.; Johnson, N. W.; Collier, M. A.; Blum, M. R.; Clendenin, N. J.; Everitt, B. J. M.; Grebe, G.; Mackars, A.; Foss, R. G.; Duch, D. S.; Bowers, S. W.; Nichol, C. A. Preclinical biochemical pharmacology and toxicology of piritrexim, a lipophilic inhibitor of dihydrofolate reductase. *Natl. Cancer Instit. Monogr.* **1987**, *5*, 111−120.
(24) Lin, J. T.; Bertino, J. R. Update on trimetrexate, a folate antagonist with antineoplastic and antiprotozoal properties. *Cancer Invest.* **1991**, *9*, 159−172.
(25) Fulton, B.; Wagstaff, A. J.; McTavish, D. Trimetrexate. A review of its pharmacodynamic and pharmacokinetic properties and therapeutic potential in the treatment of Pneumocystis carinii pneumonia. *Drugs* **1995**, *49*, 563−576.
(26) Kovacs, J. A.; Allegra, C. J.; Swan, J. C.; Drake, J. C.; Parrillo, J. E.; Chabner, B. A.; Masur, H. Potent antipneumocystis and antitoxoplasma activities of piritrexim, a lipid-soluble antifolate. *Antimicrob. Agents Chemother.* **1988**, *32*, 430−433.
(27) Queener, S. F.; Bartlett, M. S.; Jay, M. A.; Durkin, M. M.; Smith, J. W. Activity of lipid-soluble inhibitors of dihydrofolate reductase against *Pneumocystis carinii* in culture and in a rat model of infection. *Antimicrob. Agents Chemother.* **1987**, *31*, 1323−1327.
(28) Sattler, F. R.; Allegra, C. J.; Verdegem, T. D.; Akil, B.; Tuazon, C. U.; Hughlett, C.; Ogata-Arakaki, D.; Feinberg, J.; Shelhamer, J.; Lane, H. C.; Davis, R.; Boylen, C. T.; Leedom, J. M.; Masur, H. Trimetrexate-leucovorin dosage evaluation study for treatment of *Pneumocyctis carinii* pneumonia. *J. Infect. Dis.* **1990**, *161*, 91−96.
(29) Goodford, P. J. A computational procedure for determining energetically favorable binding sites on biologically important macromolecules. *J. Med. Chem.* **1985**, *28*, 849−857.
(30) Ledig, K. W. 7-(Substituted)-7H-pyrrolo[3,2-f]quinazoline-1,3-diamines. U.S. Patent 4,118,561, 1978.
(31) Jones, M. L.; Kuyper, L. F.; Styles, V. L.; Caddell, J. M. Lewis acid assisted cyclization of arylcyanoguanidines to 2,4-diaminoquinazolines. *J. Heterocycl. Chem.* **1994**, *31*, 1681−1683.
(32) Parr, W. J. E. Synthesis of selenium-containing para-phenylenediamines: Novel antidegradants for natural rubber. *J. Chem. Soc., Perkin Trans. I* **1981**, 3002−3007.
(33) Verardo, G.; Giumanini, A. G.; Strazzolini, P.; Poiana, M. Reductive N-monoalkylation of primary aromatic amines. *Synthesis* **1993**, 121−125.

(34) Kotsuki, H.; Kobayashi, S.; Matsumoto, K.; Suenaga, H.; Nishizawa, H. High Pressure Organic Chemistry; XII. A Convenient Synthesis of Aromatic Amines from Activated Aromatic Fluorides. *Synthesis* **1990**, 1147−1148.
(35) Suhr, H. Nucleophilic substitution. V. Reaction of 4-nitrofluorobenzene with primary amines. *Justus Liebigs Ann. Chem.* **1965**, *687*, 175−182.
(36) Peters, A. T.; Soboyejo, N. Iodo-substituted 4-aminoazobenzenes and 4-phenylazonaphthylamines - dyes for synthetic-polymer fibres. *J. Soc. Dyers Colour.* **1988**, *104*, 486−491.
(37) Bui, N. M.; Gillet, R.; Dumont, P. An improved synthesis of 5-iodo-2′-deoxyuridine-I131 and 5-iodouracil-I131. *Int. J. Appl. Radiat. Isot.* **1965**, *16*, 337−339.
(38) Heck, R. F. *Palladium Reagents in Organic Syntheses*; Academic Press: London, 1985.
(39) Sakamoto, T.; Kondo, Y.; Iwashita, S.; Nagano, T.; Yamanaka, H. Condensed heteroaromatic ring systems. XIII. One-step synthesis of 2-substituted 1-methylsulfonylindoles from N-(2-halophenyl)methanesulfonamides. *Chem. Pharm. Bull.* **1988**, *36*, 1305−1308.
(40) Arcadi, A.; Cacchi, S.; Marinelli, F. Palladium-catalysed coupling of aryl and vinyl triflates or halides with 2-ethynylaniline: An efficient route to functionalized 2-substituted indoles. *Tetrahedron Lett.* **1989**, *30*, 2581−2584.
(41) Blaney, J. M.; Hansch, C.; Silipo, C.; Vittoria, A. Structure-activity relationships of dihydrofolate reductase inhibitors. *Chem. Rev.* **1984**, *84*, 333−407.
(42) Champness, J. N.; Kuyper, L. F.; Beddell, C. R. Interaction between dihydrofolate reductase and certain inhibitors. In *Topics in Molecular Pharmacology*; Burgen, A. S. V., Roberts, G. C. K., Tute, M. S., Eds.; Elsevier: New York, 1986; Vol. 3, pp 335−362.
(43) Kraut, J.; Matthews, D. A. Dihydrofolate reductase. In *Biological Macromolecules and Assemblies*; Jurnak, F. A., McPherson, A., Eds.; Wiley: New York, 1987; Vol. 3, pp 1−71.
(44) Freisheim, J. H.; Matthews, D. A. The comparative biochemistry of dihydrofolate reductase. In *Folate Antagonists as Therapeutic Agents*; Sirotnak, F. M., Burchall, J. J., Ensminger, W. D., Montgomery, J. A., Eds.; Academic Press: New York, 1984; Vol. 1, pp 69−131.
(45) Champness, J. N.; Achari, A.; Ballantine, S. P.; Bryant, P. K.; Delves, C. J.; Stammers, D. K. The structure of *Pneumocystis carinii* dihydrofolate reductase to 1.9 A resolution. *Structure* **1994**, *2*, 915−924.
(46) McCormack, J. J.; Allen, B. A.; Ledig, K. W.; Hillcoat, B. L. Inhibition of dihydrofolate reductases by derivatives of 2,4-diaminopyrroloquinazoline. *Biochem. Pharmacol.* **1979**, *28*, 3227−3229.
(47) Castaldo, R. A.; Gump, D. W.; McCormack, J. J. Activity of 2,4-diaminoquinazoline compounds against *Candida* species. *Antimicrob. Agents Chemother.* **1979**, *15*, 81−86.
(48) Whitlow, M.; Howard, A. J.; Stewart, D.; Hardman, K. D.; Kuyper, L. F.; Baccanari, D. P.; Fling, M.; Tansik, R. Unpublished results.
(49) van der Bliek, A. M.; Borst, P. Multidrug resistance. *Adv. Cancer Res.* **1989**, *52*, 165−203.
(50) Gottesman, M. M.; Pastan, I. The multidrug transporter, a double-edged sword. *J. Biol. Chem.* **1988**, *263*, 12163−12166.
(51) Zamora, J. M.; Pearce, H. L.; Beck, W. T. Physical-chemical properties shared by compounds that modulate multidrug resistance in human leukemic cells. *Mol. Pharmacol.* **1988**, *33*, 454−462.
(52) Klohs, W. D.; Steinkampf, R. W.; Besserer, J. A.; Fry, D. W. Cross resistance of pleiotropically drug resistant P388 leukemia cells to the lipophilic antifolates trimetrexate and BW 301U. *Cancer Lett.* **1986**, *31*, 253−260.
(53) Assaraf, Y. G.; Molina, A.; Schimke, R. T. Cross-resistance to the lipid-soluble antifolate trimetrexate in human carcinoma cells with the multidrug-resistant phenotype. *J. Natl. Cancer Inst.* **1989**, *81*, 290−294.
(54) Selassie, C. D.; Hansch, C.; Khwaja, T. A. Structure-activity relationships of antineoplastic agents in multidrug resistance. *J. Med. Chem.* **1990**, *33*, 1914−1919.
(55) McGrath, J. P.; Varshavsky, A. The yeast STE6 gene encodes a homologue of the mammalian multidrug resistance P-glycoprotein. *Nature* **1989**, *340*, 400−404.
(56) Raymond, M.; Gros, P.; Whiteway, M.; Thomas, D. Y. Functional complementation of yeast ste6 by a mammalian multidrug resistance mdr gene. *Science* **1992**, *256*, 232−234.
(57) Cordon-Cardo, C.; O'Brien, J. P.; Casals, D.; Rittman-Grauer, L.; Biedler, J. L.; Melamed, M. R.; Bertino, J. R. Multidrug-resistance gene (P-glycoprotein) is expressed by endothelial cells at blood-brain barrier sites. *Proc. Natl. Acad. Sci. U.S.A.* **1989**, *86*, 695−698.
(58) Baccanari, D. P.; Tansik, R. L. Multiple drug resistance and its relationship to brain penetration by lipophilic dihydrofolate reductase inhibitors. *Proc. Am. Assoc. Cancer Res.* **1990**, *31*, 339.
(59) Hill, B. T.; Price, L. A. DDMP (2,4-diamino-5-(3′,4′-dichlorophenyl)-6-methylpyrimidine). *Cancer Treat. Rev.* **1980**, *7*, 95−112.
(60) Duch, D. S.; Edelstein, M. P.; Nichol, C. A. Inhibition of histamine-metabolizing enzymes and elevation of histamine levels in tissues by lipid-soluble anticancer folate antagonists. *Mol. Pharmacol.* **1980**, *18*, 100−104.
(61) Luft, B. J.; Remington, J. S. AIDS commentary; toxoplasmic encephalitis. *J. Infect. Dis.* **1988**, *157*, 1−6.
(62) Frenkel, J. K.; Hitchings, G. H. Relative reversal by vitamins (p-aminobenzoic, folic, and folinic acids) of the effects of sulfadiazine and pyrimethamine on *Toxoplasma*, mouse and man. *Antibiot. Chemother.* **1957**, *7*, 630−638.
(63) Delves, C. J.; Ballantine, S. P.; Tansik, R. L.; Baccanari, D. P.; Stammers, D. K. Refolding of recombinant *Pneumocystis carinii* dihydrofolate reductase and characterization of the enzyme. *Protein Express. Purif.* **1993**, *4*, 16−23.
(64) Hughes, W. T. Comparison of dosages, intervals, and drugs in prevention of *Pneumocystis carinii* pneumonia. *Antimicrob. Agents Chemother.* **1988**, *32*, 623−625.
(65) Ruskin, J.; LaRiviere, M. Low-dose co-trimoxazole for prevention of Pneumocystis carinii pneumonia in human immunodeficiency virus disease. *Lancet* **1991**, *337*, 468−471.
(66) Roth, B.; Strelitz, J. Z. The protonation of 2,4-diaminopyrimidines. I. Dissociation constants and substituent effects. *J. Org. Chem.* **1969**, *34*, 821−836.
(67) Cha, S. Tight-binding inhibitors - 1: Kinetic behavior. *Biochem. Pharmacol.* **1975**, *24*, 2177−2185.
(68) Henderson, P. J. F. A linear equation that describes the steady-state kinetics of enzymes and subcellular particles interacting with tightly bound inhibitors. *Biochemistry* **1972**, *127*, 321−323.
(69) Baccanari, D. B.; Joyner, S. S. Dihydrofolate reductase hysteresis and its effect on inhibitor binding analyses. *Biochemistry* **1981**, *20*, 1710−1716.
(70) Delcamp, T. J.; Susten, S. S.; Blankenship, D. T.; Freisheim, J. H. Purification and characterization of dihydrofolate reductase from methotrexate-resistant human lymphoblastoid cells. *Biochemistry* **1983**, *22*, 633−639.
(71) Krug, E. C.; Marr, J. J.; Berens, R. L. Purine metabolism in *Toxoplasma gondii*. *J. Biol. Chem.* **1989**, *264*, 10601−10607.
(72) Carmichael, J.; Mitchell, J. B.; DeGraff, W. G.; Gamson, J.; Gazdar, A. F.; Johnson, B. E.; Glatstein, E.; Minna, J. D. Chemosensitivity testing of human lung cancer cell lines using the MTT assay. *Br. J. Cancer* **1988**, *57*, 540−547.
(73) Skehan, P.; Storeng, R.; Scudiero, D.; Monks, A.; MacMahon, J.; Vistica, D.; Warren, J. T.; Bokesch, H.; Kenney, S.; Boyd, M. R. New colorimetric cytotoxicity assay for anticancer-drug screening. *J. Natl. Cancer Inst.* **1990**, *82*, 1107−1112.
(74) Ou-Yang, K.; Krug, E. C.; Marr, J. J.; Berens, R. L. Inhibition of growth of *Toxoplasma gondii* by qinghasosu and derivatives. *Antimicrob. Agents Chemother.* **1990**, *34*, 1961−1965.
(75) McLemore, T. L.; Eggleston, J. C.; Shoemaker, R. H.; Abbott, B. J.; Bohlman, M. E.; Liu, M. C.; Fine, D. L.; Mayo, J. G.; Boyd, M. R. Comparison of intrapulmonary, percutaneous intrathoracic, and subcutaneous models for the propagation of human pulmonary and nonpulmonary cancer cell lines in athymic nude mice. *Cancer Res.* **1988**, *48*, 2880−2886.
(76) Wang, A. M.; Elion, G. B.; Friedman, H. S.; Bodell, W. J.; Bigner, D. D.; Schold, S. C. Positive therapeutic interaction between thiopurines and alkylating drugs in human glioma xenografts. *Cancer Chemother. Pharmacol.* **1991**, *27*, 278−284.
(77) Comley, J. C. W.; Sterling, A. M. Artificial infections of *Pneumocystis carinii* in the SCID mouse and their use in the *in vivo* evaluation of antipneumocystis drugs. *J. Eukaryot. Microbiol.* **1994**, *41*, 540−546.
(78) Comley, J. C. W.; Sterling, A. M. Effect of atovaquone and atovaquone drug combinations on prophylaxis of *Pneumocystis carinii* Pneumonia in SCID mice. *Antimicrob. Agents Chemother.* **1995**, *39*, 806−811.
(79) Foss, R. G.; Sigel, C. W. Lipid-soluble inhibitors of DHFR. III: Quantitative thin-layer and high performance liquid chromatographic methods of the measurement of plasma concentrations of the antifolate, 2,4-diamino-6-(2,5-dimethoxybenzyl)-5-methylpyrido[2,3-d]pyrimidine. *J. Pharm. Sci.* **1982**, *71*, 1176−1178.

JM9505122